# Spin-s Spin-Glass Phases in the d=3 Ising Model

E. Can Artun[1] and A. Nihat Berker[1,2]

[1] *Faculty of Engineering and Natural Sciences, Kadir Has University, Cibali, Istanbul 34083, Turkey*
[2] *Department of Physics, Massachusetts Institute of Technology, Cambridge, Massachusetts 02139, USA*

All higher-spin ($s \geq 1/2$) Ising spin glasses are studied by renormalization-group theory in spatial dimension $d = 3$. The s-sequence of global phase diagrams, the chaos Lyapunov exponent, and the spin-glass runaway exponent are calculated. It is found that, in $d = 3$, a finite-temperature spin-glass phase occurs for all spin values, including the continuum limit of $s \to \infty$. The phase diagrams, with increasing spin $s$, saturate to a limit value. The spin-glass phase, for all $s$, exhibits chaotic behavior under rescalings, with the calculated Lyapunov exponent of $\lambda = 1.93$ and runaway exponent of $y_R = 0.24$, showing simultaneous strong-chaos and strong-coupling behaviors. The ferromagnetic-spinglass-antiferromagnetic phase transitions occurring around $p_t = 0.37$ and 0.63 are unaffected by $s$, confirming the percolative nature of this phase transition.

## I. INTRODUCTION: SPIN-S ISING SPIN-GLASS SYSTEMS

Frozen disorder of the interactions introduces many qualitatively and quantitatively new effects to statistical mechanical systems, such as the immediate (i.e., with infinitesimal disorder) conversion of first-order phase transitions into second-order phase transitions [1–4] or the creation of an entirely new phase such as the spin-glass phase [5]. The latter occurs under frozen (quenched) competing interactions causing local minimum-energy degeneracies dubbed frustration [6]. The signature of the spin-glass phase is the appearance of a chaotic sequence of interactions [7–17] under the successive scale changes of a renormalization-group transformation. This translates to a chaotic spin-spin correlation function, as function of distance, at a given scale.[18] The spin-glass phase and its rescaling chaos appears with the introduction, by rewiring, of infinitesimal frustration to the Mattis phase [19] obtained by random local spin redefinitions (gauge transformations) in the usual ferromagnetic or antiferromagnetic phase.[20] On the other hand, strong chaos, signalled by a large Lyapunov exponent, of the spin-glass phase in fully frustated systems continues [25] until the lower-critical dimension $d_c \simeq 2.5$ of the spin-glass phase [21–27]. Thus both gradual [20] or abrupt [25] onsets of chaos are seen.

Most spin-glass studies have been on the classical spin $s = 1/2$ Ising model, where locally $s_i = \pm 1$.[29] Spin-glass studies have also been done on $q$-state clock models and their continuum limit the XY model [30, 31], chiral (helical [32]) Potts and clock models, in fact leading to a chiral spin-glass Potts [33] and clock [34, 35] phases, and quantum Heisenberg models [36]. The position-space renormalization-group method appears to be a method suited for such studies, where the rescaling behavior of the distribution of the quenched random interactions is followed and analyzed [37]. This is best effected (Fig. 2) by use of the Migdal-Kadanoff approximation [38, 39] or, equivalently, the exact recursion of a hierarchical lattice [40–43]. In the current work, we quantitatively and globally study, in spatial dimension $d = 3$, the Ising spin glass for all spins $s = 1/2, 1, 3/2, 2, 5/2, ...$ to the limiting value $s \to \infty$, obtaining the global $s$-sequence phase diagram (Fig. 1) and chaotic behaviors.

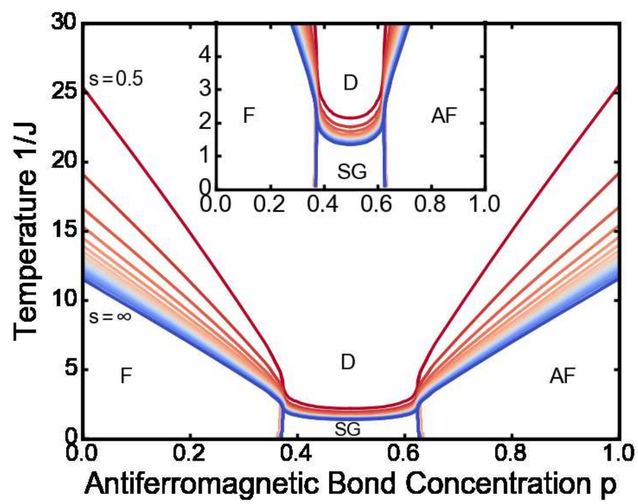


FIG. 1. Calculated phase diagrams of the spin-$s$ Ising spin glasses in $d = 3$. Fom top to bottom, $s = 1/2, 1, 3/2, 2, 5/2, 3, ...$ to $s \to \infty$. There is an accumulation, from above, of the phase diagrams at the lowermost, but still at finite-temperature, phase diagram of the continuum limit $s \to \infty$.

The spin-$s$ Ising model is defined by the Hamiltonian

$$-\beta\mathcal{H} = \sum_{\langle ij \rangle} J_{ij}(s_i/s)(s_j/s)\,, \tag{1}$$

where $\beta = 1/kT$, at each site $i$ of the lattice the spin $s_i = \pm 1/2, \pm 1, \pm 3/2, ..., \pm s$, and $\langle ij \rangle$ denotes summation over all nearest-neighbor site pairs. The division by $s$ is done to conserve the energy scale across the different spin-$s$ models and thereby make meaningful temperature comparisons between them. Note that for $s = 1/2$, this formalism yields the much studied $s_i/s = \pm 1$ case. The bond $J_{ij}$ is ferromagnetic $+J > 0$ or antiferromagnetic $-J$ with respective probabilities $1-p$ and $p$. Under renormalization-group tranformation, this "double-delta" distribution of interactions is not conserved. A more complicated distribution of interactions ensues and is kept track of, as explained below.

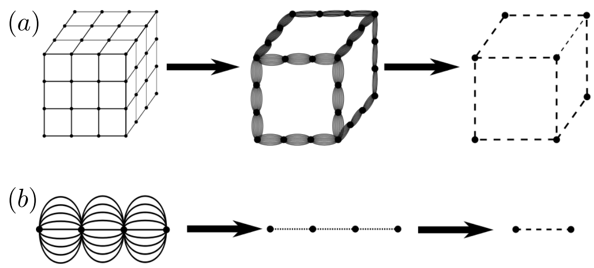


FIG. 2. (a) Migdal-Kadanoff approximate renormalization-group transformation for the $d = 3$ cubic lattice with the length-rescaling factor of $b = 3$. In this intuitive approximation, bond moving is followed by decimation. (b) Exact renormalization-group transformation of the $d = 3, b = 3$ hierarchical lattice for which the Migdal-Kadanoff renormalization-group recursion relations are exact. The construction of a hierarchical lattice proceeds in the opposite direction of its renormalization-group solution. From [34, 40].

## II. METHOD: RENORMALIZATION-GROUP FLOWS OF THE QUENCHED PROBABILITY DISTRIBUTION OF THE INTERACTIONS

Under renormalization group, for $s > 1/2$, the Hamiltonian does not conserve its form in Eq.(1). Thus, for any $s$, the Hamiltonian is most generally expressed as

$$-\beta\mathcal{H} = \sum_{\langle ij \rangle} E(s_i, s_j)\,, \tag{2}$$

With no loss of generality, for each $< ij >$, the same constant is subtracted from all terms $E(s_i, s_j)$, so that the largest energy $E(s_i, s_j)_{max}$ of the spin-spin interaction is zero (and all other $E(s_i, s_j) < 0$). This formulation makes it possible to follow global renormalization-group trajectories, necessary for the calculation of phase boundaries, Lyapunov exponent, and runaway exponent, without running into numerical overflow problems. As the local renormalization-group transformation, the Migdal-Kadanoff approximate transformation [38, 39] and, equivalently, the exact transformation for the $d = 3$ hierarchical lattice [40–42] is used (Fig. 2). Recent works using exactly soluble hierarchical models are in Refs. [44–52]. The length rescaling factor of $b = 3$ is used, to preserve under renormalization group the ferromagnetic-antiferromagnetic symmetry of the system. This local transformation consists in bond moving followed by decimation, with the above-mentioned subtraction after each local bond moving and decimation, giving the local renormalized energies $E'(s_i, s_j) \leq 0$. In our notation, all renormalized quantities are designated by a prime.

The quenched randomness is included by keeping, as a distribution, 10000 sets of the nearest-neighbor interaction energies $E(s_i, s_j)$. At the beginning of each renormalization-group trajectory, this distribution is formed from the double-delta distribution characterized by interactions $\pm J$ with probabilities $p, (1 - p)$. 10000 local renormalization-group transformations determine each subsequent distribution as explained below.

The local renormalization-group transformation is simply expressed in terms of the transfer matrix $T(s_i, s_j) = e^{E(s_i,s_j)}$: Bond moving consists of multiplying elements at the same position of $b^{d-1} = 9$ transfer matrices randomly chosen from the distribution,

$$\widetilde{T}(s_i, s_j) = \prod_{k=1}^{9} T_k(s_i, s_j)\,, \tag{3}$$

so that a distribution of 10000 bond-moved transfer matrices is generated. Decimation consists of matrix multiplication of three randomly chosen bond-moved transfer matrices,

$$\mathbf{T'} = \widetilde{\mathbf{T}}_\mathbf{1} \cdot \widetilde{\mathbf{T}}_\mathbf{2} \cdot \widetilde{\mathbf{T}}_\mathbf{3}\,, \tag{4}$$

so that a distribution of 10000 renormalized transfer matrices is generated. Phases are determined by following trajectories to their asymptotic limit: The asymptotic limit transfer matrices of trajectories starting in the ferromagnetic phase all have 1 in the corner diagonals and 0 at all other positions. The asymptotic limit transfer matrices of trajectories starting in the antiferromagnetic phase all have 1 in the corner anti-diagonals and 0 at all other positions. The asymptotic limit transfer matrices of trajectories starting in the spin-glass phase all have 1 in the corner diagonals and anti-diagonals, and 0 at all other positions. The asymptotic limit transfer matrices of trajectories starting in the disordered phase all have 1 at all other positions. Phase diagrams are obtained by numerically determining the boundaries, in the unrenormalized system, of these asymptotic flows.

## III. RESULTS: GLOBAL S-SEQUENCE PHASE DIAGRAM AND SATURATION

The calculated phase diagrams of the spin-$s$ Ising spin glasses in $d = 3$ are shown in Fig. 1. Fom top to bottom, the phase diagrams are for spin-$s = 1/2, 1, 3/2, 2, 5/2, 3, ...$ to $s \to \infty$. There is an accumulation, from above, of the phase diagrams at the lowermost, but still at finite-temperature, phase diagram of the continuum limit $s \to \infty$.

The calculated ferromagnetic (at $p = 0$) and spin-glass (at $p = 0.5$) phase transition temperatures as a function of spin value $s$ are given in Fig. 3. With increasing $s$ both transition temperatures saturate around $s \simeq 4$. A similar behavior was found in $q$-state clock models saturating at the continuum XY model transition temperature.[43]

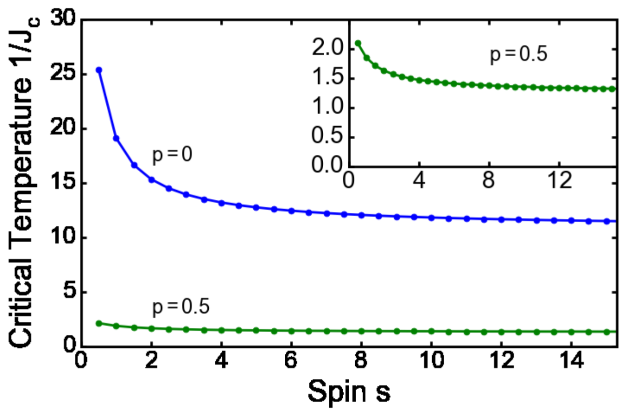


FIG. 3. The calculated ferromagnetic (at $p = 0$) and spin-glass (at $p = 0.5$) phase transition temperatures as a function of spin value $s$. Note that with increasing $s$ both transition temperatures saturate around $s \simeq 4$. A similar behavior was found in $q$-state clock models.[43]

## IV. RESULTS: CHAOS FOR ALL SPINS S, LYAPUNOV EXPONENT AND RUNAWAY EXPONENT

For all spin-$s$, the renormalization-group trajectories starting within the spin-glass phase are asymptotically chaotic, as seen in Fig. 4, where the consecutively renormalized (combining with neighboring interactions) values at a given location $< ij >$ are followed. For the interaction $K_{ij}$, we have used the difference between the largest value (which is 0 by construction) and the lowest value in $E(s_i, s_j)$. $\overline{K}$ is the average of this interaction over the entire distribution at the given renormalization-group step. The chaotic behavior is strong, as measured by the Lyapunov exponent [53, 54]

$$\lambda = \lim_{n\to\infty} \frac{1}{n} \sum_{k=0}^{n-1} \ln \left| \frac{dx_{k+1}}{dx_k} \right| , \qquad (5)$$

where $x_k = K_{ij}/\overline{K}$ at step $k$ of the renormalization-group trajectory. Eliminating the first 100 renormalization-group steps as crossover from initial conditions to asymptotic behavior and using the next 1500 steps, Eq.(5) yielded $\lambda = 1.93$ for all spins $s$.

In addition to strong chaos, the renormalization-group trajectories show asymptotic strong coupling behavior,

$$\overline{K'} = b^{y_R}\, \overline{K} , \qquad (6)$$

where $y_R > 0$ is the runaway exponent [25]. Again using 1500 renormalization-group steps after discarding 100 steps, we find $y_R = 0.24$ for all spins $s$. Note that this is a "weak" strong coupling behavior, as the stronger runaway exponent of the ferromagnetic and antiferromagnetic phases is $y_R = d - 1 = 2$.

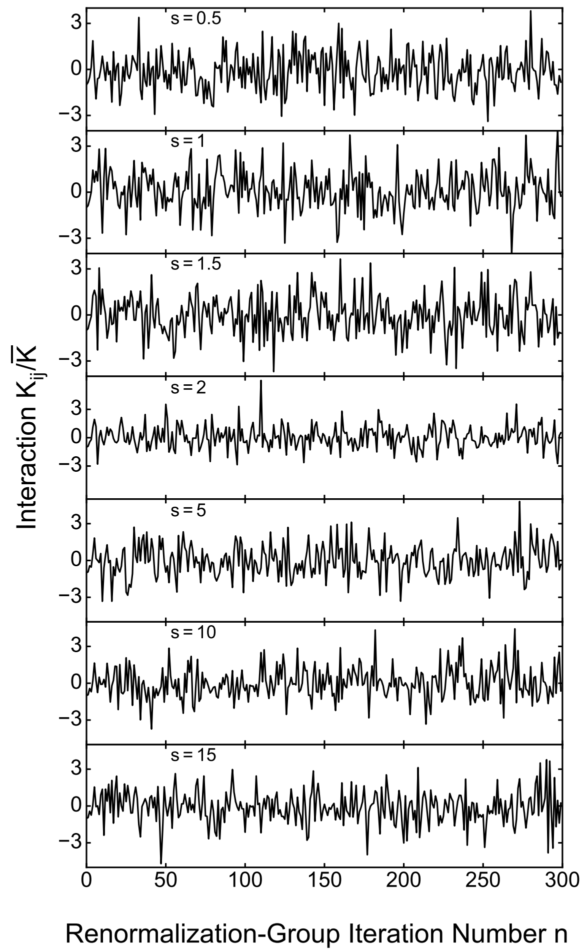


FIG. 4. The chaotic renormalization-group trajectory of the interaction $K_{ij}$ at a given location $< ij >$, for various spin $s$ values, at spatial dimension $d = 3$. Note the strong chaotic behavior for all $s$, as also reflected by the calculated Lyapunov exponent $\lambda = 1.93$ for all $s$. The calculated runaway exponent is $y_R = 0.24$ for all $s$, showing simultaneous strong-chaos and strong-coupling behaviors.

## V. CONCLUSION

We have calculated the global spin-$s$ sequence of phase diagrams for all spins $s = 1/2, 1, 3/2, 2, 5/2, 3, ..., s \to \infty$ for the Ising spin-glass system in spatial dimension $d = 3$. The phase diagrams, all with a finite-temperature spin-glass phase, for increasing spin $s$ saturate to the limit value of $s \to \infty$. For all spins $s$, the spin-glass phase has renormalization-group trajectories that are chaotic, with calculated Lyapunov exponent $\lambda = 1.93$ and runaway exponent $y_R = 0.24$, thus simultaneously showing strong chaotic and "weak" strong-coupling behaviors.

**ACKNOWLEDGMENTS**

Support by the Kadir Has University Doctoral Studies Scholarship Fund and by the Academy of Sciences of Turkey (TÜBA) is gratefully acknowledged.


[1] M. Aizenman and J. Wehr, Rounding of First-Order Phase Transitions in Systems with Quenched Disorder, Phys. Rev. Lett. **62**, 2503 (1989).

[2] M. Aizenman and J. Wehr, Phys. Rev. Lett. **64**, 1311(E) (1990).

[3] K. Hui and A. N. Berker, Random-Field Mechanism in Random-Bond Multicritical Systems, Phys. Rev. Lett. **62**, 2507 (1989).

[4] K. Hui and A. N. Berker, erratum, Phys. Rev. Lett. **63**, 2433 (1989).

[5] S.F. Edwards and P. W. Anderson, Theory of Spin Glasses, J. Phys. F **5**, 965 (1975).

[6] G. Toulouse, Theory of Frustration Effect in Spin Glasses 1., Commun. Phys. **2**, 115 (1977).

[7] S. R. McKay, A. N. Berker, and S. Kirkpatrick, Spin-Glass Behavior in Frustrated Ising Models with Chaotic Renormalization-Group Trajectories, Phys. Rev. Lett. **48**, 767 (1982).

[8] S. R. McKay, A. N. Berker, and S. Kirkpatrick, Amorphously Packed, Frustrated Hierarchical Models: Chaotic Rescaling and Spin-Glass Behavior, J. Appl. Phys. **53**, 7974 (1982).

[9] A. N. Berker and S. R. McKay, Hierarchical Models and Chaotic Spin Glasses, J. Stat. Phys. **36**, 787 (1984).

[10] E. J. Hartford and S. R. McKay, Ising Spin-Glass Critical and Multicritical Fixed Distributions from a Renormalization-Group Calculation with Quenched Randomness, J. Appl. Phys. **70**, 6068 (1991).

[11] Z. Zhu, A. J. Ochoa, S. Schnabel, F. Hamze, and H. G. Katzgraber, Best-Case Performance of Quantum Annealers on Native Spin-Glass Benchmarks: How Chaos Can Affect Success Probabilities, Phys. Rev. A **93**, 012317 (2016).

[12] W. Wang, J. Machta, and H. G. Katzgraber, Bond Chaos in Spin Glasses Revealed through Thermal Boundary Conditions, Phys. Rev. B **93**, 224414 (2016).

[13] L. A. Fernandez, E. Marinari, V. Martin-Mayor, G. Parisi, and D. Yllanes, Temperature Chaos is a Non-Local Effect, J. Stat. Mech. - Theory and Experiment, 123301 (2016).

[14] A. Billoire, L. A. Fernandez, A. Maiorano, E. Marinari, V. Martin-Mayor, J. Moreno-Gordo, G. Parisi, F. Ricci-Tersenghi, J.J. Ruiz-Lorenzo, Dynamic Variational Study of Chaos: Spin Glasses in Three Dimensions, J. Stat. Mech. - Theory and Experiment, 033302 (2018).

[15] W. Wang, M. Wallin, and J. Lidmar, Chaotic Temperature and Bond Dependence of Four-Dimensional Gaussian Spin Glasses with Partial Thermal Boundary Conditions, Phys. Rev. E **98**, 062122 (2018).

[16] R. Eldan, The Sherrington-Kirkpatrick Spin Glass Exhibits Chaos, J. Stat. Phys. **181**, 1266 (2020).

[17] M. Baity-Jesi, E. Calore, A. Cruz, L. A. Fernandez, J. M. Gil-Narvion, I. G.-A. Pemartin, A. Gordillo-Guerrero, D. Iñiguez, A. Maiorano, E. Marinari, V. Martin-Mayor, J. Moreno-Gordo, A. Muñoz-Sudupe, D. Navarro, I. Paga, G. Parisi, S. Perez-Gaviro, F. Ricci-Tersenghi, J. J. Ruiz-Lorenzo, S. F. Schifano, B. Seoane, A. Tarancon, R. Tripiccione, and D. Yllanes, Temperature Chaos Is Present in Off-Equilibrium Spin-Glass Dynamics, Comm. Phys. **4**, 74 (2021).

[18] N. Aral and A. N. Berker, Chaotic Spin Correlations in Frustrated Ising Hierarchical Lattices, Phys. Rev. B **79**, 014434 (2009).

[19] D. C. Mattis, Solvable Spin Systems with Random Interactions, Phys. Lett. A **56**, 421 (1976).

[20] E. Ilker and A. N. Berker, Overfrustrated and Underfrustrated Spin Glasses in d=3 and 2: Evolution of Phase Diagrams and Chaos including Spin-Glass Order in d=2, Phys. Rev. E **89**, 042139 (2014).

[21] S. Franz, G. Parisi, and M.A. Virasoro, Interfaces and Lower Critical Dimension in a Spin-Glass Model, J. Physique I **4**, 1657 (1994).

[22] C. Amoruso, E. Marinari, O. C. Martin, and A. Pagnani, Scalings of Domain Wall Energies in Two Dimensional Ising Spin Glasses, Phys. Rev. Lett. **91**, 087201 (2003).

[23] J.-P. Bouchaud, F. Krzakala, and O. C. Martin, Energy Exponents and Corrections to Scaling in Ising Spin Glasses, Phys. Rev. B **68**, 224404 (2003).

[24] S. Boettcher, Stiffness of the Edwards-Anderson Model in All Dimensions, Phys. Rev. Lett. **95**, 197205 (2005).

[25] M. Demirtaş, A. Tuncer, and A. N. Berker, Lower-Critical Spin-Glass Dimension from 23 Sequenced Hierarchical Models, Phys. Rev. E 92, 022136 (2015).

[26] A. Maiorano and G. Parisi, Support for the Value 5/2 for the Spin Glass Lower Critical Dimension at Zero Magnetic Field, Proc. Natl. Acad. Sci. USA **115**, 5129 (2018).

[27] B. Atalay and A. N. Berker, A Lower Lower-Critical Spin-Glass Dimension from Quenched Mixed-Spatial-Dimensional Spin Glasses, Phys. Rev. E 98, 042125 (2018).

[28] G. Grinstein, A. N. Berker, J. Chalupa, and M. Wortis, Exact Renormalization Group with Griffiths Singularities and Spin-Glass Behavior: The Random Ising Chain, Phys. Rev. Lett. **36**, 1508 (1976).

[29] I. Morgenstern and K. Binder, Evidence against Spin-Glass Order in the 2-Dimensional Random-Bond Ising Model, Phys. Rev. Lett. 43, 1615 (1979).

[30] E. Ilker and A. N. Berker, High q-State Clock Spin Glasses in Three Dimensions and the Lyapunov Exponents of Chaotic Phases and Chaotic Phase Boundaries, Phys. Rev. E **87**, 032124 (2013).

[31] E. Ilker and A. N. Berker, Odd q-State Clock Spin-Glass Models in Three Dimensions, Asymmetric Phase Diagrams, and Multiple Algebraically Ordered Phases, Phys. Rev. E **90**, 062112 (2014).

[32] M. Kardar and A. N. Berker, Commensurate-Incommensurate Phase Diagrams for Overlayers from a Helical Potts Model, Phys. Rev. Lett. **48**, 1552 (1982).

[33] T. Çağlar and A. N. Berker, Chiral Potts Spin Glass in d = 2 and 3 Dimensions, Phys. Rev. E **94**, 032121 (2016).

[34] T. Çağlar and A. N. Berker, Devil's Staircase Continuum in the Chiral Clock Spin Glass with Competing Ferromagnetic-Antiferromagnetic and Left-Right Chiral Interactions, Phys. Rev. E **95**, 042125 (2017).

[35] T. Çağlar and A. N. Berker, Phase Transitions Between Different Spin-Glass Phases and Between Different Chaoses in Quenched Random Chiral Systems, Phys. Rev. E **96**, 032103 (2017).

[36] C. N. Kaplan and A. N. Berker, Quantum-Mechanically Induced Asymmetry in the Phase Diagrams of Spin-Glass Systems, Phys. Rev. Lett. 100, 027204, 1-4 (2008).

[37] D. Andelman and A. N. Berker, Scale-Invariant Quenched Disorder and its Stability Criterion at Random Critical Points, Phys. Rev. B **29**, 2630 (1984).

[38] A. A. Migdal, Phase Transitions in Gauge and Spin Lattice Systems, Zh. Eksp. Teor. Fiz. **69**, 1457 (1975) [Sov. Phys. JETP **42**, 743 (1976)].

[39] L. P. Kadanoff, Notes on Migdal's Recursion Formulas, Ann. Phys. (N.Y.) **100**, 359 (1976).

[40] A. N. Berker and S. Ostlund, Renormalisation-Group Calculations of Finite Systems: Order Parameter and Specific Heat for Epitaxial Ordering, J. Phys. C **12**, 4961 (1979).

[41] R. B. Griffiths and M. Kaufman, Spin Systems on Hierarchical Lattices: Introduction and Thermodynamic Limit, Phys. Rev. B **26**, 5022R (1982).

[42] M. Kaufman and R. B. Griffiths, Spin Systems on Hierarchical Lattices: 2. Some Examples of Soluble Models, Phys. Rev. B **30**, 244 (1984).

[43] E. C. Artun and A. N. Berker, Complete Density Calculations of q-State Potts and Clock Models: Reentrance of Interface Densities under Symmetry Breaking, Phys. Rev. E **102**, 062135 (2020).

[44] A. V. Myshlyavtsev, M. D. Myshlyavtseva, and S. S. Akimenko, Classical Lattice Models with Single-Node Interactions on Hierarchical Lattices: The Two-Layer Ising Model, Physica A **558**, 124919 (2020).

[45] M. Derevyagin, G. V. Dunne, G. Mograby, and A. Teplyaev, Perfect Quantum State Transfer on Diamond Fractal Graphs, Quantum Information Processing, **19**, 328 (2020).

[46] S.-C. Chang, R. K. W. Roeder, and R. Shrock, q-Plane Zeros of the Potts Partition Function on Diamond Hierarchical Graphs, J. Math. Phys. **61**, 073301 (2020).

[47] C. Monthus, Real-Space Renormalization for Disordered Systems at the Level of Large Deviations, J. Stat. Mech. - Theory and Experiment, 013301 (2020).

[48] O. S. Sarıyer, Two-Dimensional Quantum-Spin-1/2 XXZ Magnet in Zero Magnetic Field: Global Thermodynamics from Renormalisation Group Theory, Philos. Mag. **99**, 1787 (2019).

[49] P. A. Ruiz, Explicit Formulas for Heat Kernels on Diamond Fractals, Comm. Math. Phys. **364**, 1305 (2018).

[50] M. J. G. Rocha-Neto, G. Camelo-Neto, E. Nogueira, Jr., and S. Coutinho, The Blume–Capel Model on Hierarchical Lattices: Exact Local Properties, Physica A **494**, 559 (2018).

[51] F. Ma, J. Su, Y. X. Hao, B. Yao, and G. G. Yan, A Class of Vertex–Edge-Growth Small-World Network Models Having Scale-Free, Self-Similar and Hierarchical Characters Physica A **492**, 1194 (2018).

[52] S. Boettcher and S. Li, Analysis of Coined Quantum Walks with Renormalization, Phys. Rev. A **97**, 012309 (2018).

[53] P. Collet and J.-P. Eckmann, *Iterated Maps on the Interval as Dynamical Systems* (Birkhäuser, Boston, 1980).

[54] R. C. Hilborn, *Chaos and Nonlinear Dynamics*, 2nd ed. (Oxford University Press, New York, 2003).